



Evolution from non-Griffiths phase to Griffiths phase: Giant enhancement of magnetoresistance in nanocrystalline $(\text{La}_{0.4}\text{Y}_{0.6})_{0.7}\text{Ca}_{0.3}\text{MnO}_3$ compound

Sanjib Banik ^{a,*}, Nasrin Banu ^b, I. Das ^a

^a Condensed Matter Physics Division, Saha Institute of Nuclear Physics, HBNI, 1/AF-Bidhannagar, Kolkata 700 064, India

^b Department of Materials Science, Indian Association for the Cultivation of Science, 2A & 2B Raja S. C. Mullick Road, Jadavpur, Kolkata 700 032, India

ARTICLE INFO

Article history:

Received 5 January 2018
Received in revised form
16 February 2018
Accepted 19 February 2018
Available online 22 February 2018

Keywords:

Magnetoresistance
Griffiths phase
Non-Griffiths phase
Magnetization

ABSTRACT

The particle size driven modification of the non-Griffiths phase to Griffiths phase in $(\text{La}_{0.4}\text{Y}_{0.6})_{0.7}\text{Ca}_{0.3}\text{MnO}_3$ (LYCMO) compound have been presented here. In the nanocrystal, the decreased lattice distortions together with the quenched disorder arising from the ionic size mismatch of the different A-site ions are the possible reason for the occurrence of Griffiths phase. On the other hand, though in the bulk compound quenched disorder is present but the higher distortions enhance the effective antiferromagnetic superexchange interactions and may be the probable reason for the non-Griffiths phase which is identified by the upturn of the inverse susceptibility versus temperature plot from the Curie-Weiss line. An enhancement of Colossal magnetoresistance (CMR) in the minimal surface disorder nanoparticle ($\sim 120\text{nm}$) has been observed. The study shows that for LYCMO compound, the enhancement of CMR in 120 nm nanoparticle is due to the conversion from non-Griffiths phase to Griffiths phase.

© 2018 Elsevier B.V. All rights reserved.

1. Introduction

The observation of Griffiths singularities [1] in materials exhibiting complex magnetic interactions has drawn notable scientific interest [2–5]. Griffiths pointed out that, for a magnetic system, the quenched random distribution makes the thermodynamic function unanalytic in the temperature range $T_C < T < T_G$, where T_G represents the characteristic temperature below which ferromagnetic clusters start to nucleate and T_C is the ferromagnetic ordering temperature. This temperature regime $T_C < T < T_G$ is the Griffiths phase (GP) which is microscopically characterized by a short-range ferromagnetic cluster like system induced by quenched disorder. The signature of GP is visualized experimentally from the anomalies in magnetic susceptibility and heat capacity data [6–8]. The GP behavior has been observed in various systems including spin glass systems [9], heavy fermi materials [7,8], layer manganites [10] and hole-doped manganites [11–13,15]. Burgy [16] has pointed out that the coexistence of competing ferromagnetic (FM) and antiferromagnetic (AFM) phases can also exhibit GP phase. Thus the main ingredients for GP observation are the competition between

magnetic interactions and the intrinsic disorder. However, depending upon the dominance of AFM interactions system can also exhibit a non-Griffiths like phase which is identified by an upturn from the Curie-Weiss law $\chi^{-1} \propto (T - \theta_p)$ behavior in $\chi^{-1}(T)$ data above the Curie temperature. Currently, a non-Griffiths like phase has been observed in various systems with competing FM-AFM interactions such as cobaltites [19], manganites [17,18], double perovskites [20] etc. Therefore, depending upon the relative strength of FM and AFM interactions system may behave non-Griffiths phase or Griffiths phase. Recently, there is an ongoing debate [10,13] on the concurrence of GP and CMR. However, the effect of the modification of non-Griffiths phase to Griffiths phase and its effect on CMR property has rarely been addressed. Very recently, a non-Griffiths like phase has been observed in bulk polycrystalline $(\text{La}_{1-x}\text{Y}_x)_{0.7}\text{Ca}_{0.3}\text{MnO}_3$ compounds with ‘Y’ doping, where field induced modification is observed up to the doping range $x < 0.6$ [14]. However, investigations on the reduction of particle sizes in the $(\text{La}_{1-x}\text{Y}_x)_{0.7}\text{Ca}_{0.3}\text{MnO}_3$ compounds are ignored.

In this article, we report the observation of Griffiths phase in nanocrystalline $(\text{La}_{0.4}\text{Y}_{0.6})_{0.7}\text{Ca}_{0.3}\text{MnO}_3$ compound via magnetization, electrical transport and heat capacity measurements. Our study implies that the origin of Griffiths phase is associated with the release of lattice distortions. The study reveals that occurrence

* Corresponding author.

E-mail address: sanjib.banik@saha.ac.in (S. Banik).

of Griffiths phase is also associated with the enhancement of colossal magnetoresistance (CMR) in the nanocrystalline samples.

2. Results and discussion

2.1. Structural characterization

The room temperature XRD data (Fig. 1) of all the polycrystalline samples have been analyzed by Rietveld profile fitting using FULLPROF software. The Rietveld profile fitting of the XRD data shows the single phase nature of all the samples with 'Pnma' space group. The mean crystallite sizes has been calculated from x-ray line width broadening using Scherrer equation and the average particle sizes has been determined from SEM measurements. The obtained crystallite sizes are less than the particle sizes of the nanoparticles as nanoparticles comprise surface disorder which does not contribute to the XRD pattern. The average particle size of the bulk sample from SEM measurements comes out to be ~ 1000 nm. For convenience, hereafter bulk sample will be referred as 'Bulk' whereas nanocrystallite samples will be referred as 'Nano1' (average particle size 120 nm), 'Nano2' (average particle size 80 nm) and 'Nano3' (average particle size 65 nm) respectively.

From the extracted lattice parameters a , b and c the modification of orthorhombic distortions, defined as $\Delta(\perp) = \frac{a+b-c/\sqrt{2}}{a+b+c/\sqrt{2}}$ and $\Delta(\parallel) = \frac{a-b}{a+b}$ has been compared for bulk and nanocrystallite samples. The

distinct reduction of $\Delta(\perp)$ is observed with decreasing particle sizes and the same happens for $\Delta(\parallel)$ also (Fig. 2(b)), though there is a little increase when particle size decreases from 120 nm. The decrease of $\Delta(\perp)$ and $\Delta(\parallel)$ is also perceptible from the decrease of the angle between (200) and (121) planes with the decrease of particle size. As crystal lattice is susceptible to have higher symmetry with reduction of particle sizes [21], decrease in distortions in nanocrystallite samples is expected. The unit cell volume has also decreased with the reduction of particle size (Fig. 2(a)) which may be due to the enhanced surface pressure.

The temperature dependence of XRD measurements of 'Bulk' and 'Nano1' has also been performed. The unit cell volume of 'Bulk' decreases with decreasing temperature and it is expected because of the reduction of lattice vibrations. On the other hand in case of 'Nano1' there is a sudden decrease of unit cell volume around 250 K, below which there is a gradual decrease of the unit cell volume. Although there is no structural phase transition around 250 K. The calculated distortions $\Delta(\perp)$ and $\Delta(\parallel)$ has been compared for 'Bulk' and 'Nano1' samples in the temperature ranges 20–300 K. With decreasing temperature, enhancement of $\Delta(\perp)$ and $\Delta(\parallel)$ is observed. Though in 'Nano1' these distortions are small in the whole temperature range compared with the bulk sample.

2.2. Electrical transport and magnetotransport study

The evolution of distortions from bulk to nanocrystallite greatly influence the electrical transport and magnetotransport properties. The temperature dependence of resistivity [$\rho(T)$] of all the polycrystalline samples has been carried out in the absence and in the presence of 90 kOe external magnetic field. The measurements were performed during warming cycle from 2 to 300 K after cooling the samples in zero magnetic field. The temperature dependence of zero field resistivity data shows the insulating nature of all the samples down to measurable temperature limit as shown in Fig. 3. Compared to the 'Bulk' sample resistivity value decreases for the 'Nano1' sample. However, for the consecutive nanoparticles the value of resistivity increases from the 'Nano1' sample. Usually, with the reduction of particle sizes, the decrease of resistivity is observed in charge-ordered compound due to the growth of surface ferromagnetism [22] and enhancement of resistivity occurs in case of ferromagnetic compound due to the enhanced surface disorder [23]. In the present case, initial size reduction (from $\sim \mu\text{m}$ to 120 nm) suppress the resistivity and further reduction enhances it. This feature indicates that there are two competing features, one is surface disorder and other is related to the change in the structural parameter from bulk to 'Nano1'. In 'Nano1' sample reduction of distortions is observed which is one of the competing features playing the role in huge reduction of resistivity with initial particle size reduction. On application of 90 kOe external magnetic field suppression of resistivity is observed in all the nanoparticles but a huge change of $\sim 10^5$ order near 50 K temperature is observed in 'Nano1' sample. The field induced metal-insulator transition is observed in 'Nano1' particle around 75 K and in 'Nano2' it is around 60 K but no signature of metallic transition is visible in 'Nano3'. This decrease of T_{MI} with the reduction of particle sizes is due to the lowering phase fraction responsible for conduction. In 'Nano1' at low temperature (< 25 K) there is an upturn in resistivity and this upturn increases with lowering particle sizes. It implies the dominating feature of surface contribution from 'Nano2' particle.

From the magnetotransport study, the variation of magnetoresistance ($MR\%$) with temperature in bulk and nanocrystallite samples has been performed. The $MR\%$ has been calculated using $MR(\%) = \frac{R(H) - R(0)}{R(0)} \times 100$ which is commonly used for CMR materials and here where $R(H)$ is the resistance in presence of magnetic field

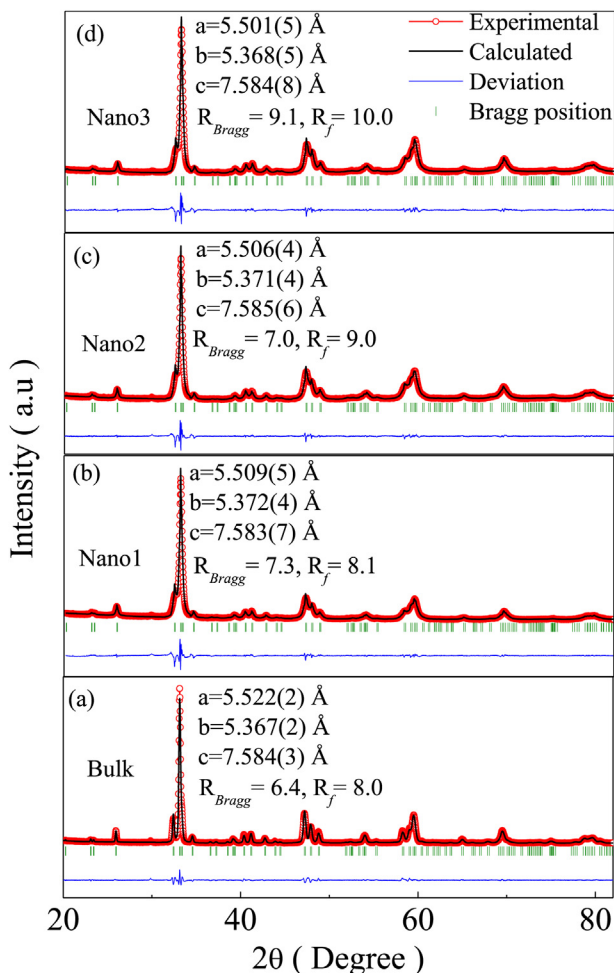


Fig. 1. Room temperature XRD data along with profile fitted data for (a) Bulk (b) Nano1 (c) Nano2 and (d) Nano3 sample.

Download English Version:

<https://daneshyari.com/en/article/7992965>

Download Persian Version:

<https://daneshyari.com/article/7992965>

[Daneshyari.com](https://daneshyari.com)